Modeling Cell Adhesion Forces on a Nanopatterned Surface

Peter Gu, Sibley School of Mechanical and Aerospace Engineering, Cornell University, Ithaca, NY

Nanoscale patterns covered with fibronectin allow attachment and characterization of individual cells. Of particular importance is the adhesive force between the cells integrin based focal adhesions (FA) and the extracellular matrix (ECM). Such a force not only anchors the cell to its surroundings, but is also involved in signal transduction pathways that regulate tissue growth and repair. Previously, it was found that on a nanopattern, there is a minimum area in which cells can produce stable bonds to a surface. I created a mathematical model to predict the adhesive force generated by a cell onto a surface with nanoscale geometry. This model involved equilibrating the forces and moments on a cell that barely adheres when exposed to a fluid shear flow. In this case, the shear stress on the cell is equal to the adhesion strength, the stress level that would cause half of the exposed cells to detach on average. The resulting forces were compared to those measured in previous studies using the same nanopattern. The model is in good agreement with the results, with some deviations for patterns with areas close to the minimum. Another task was to create designs for new nanopatterns to be used in future studies with individually separated cells. These designs were created in AutoCAD and fit into a circular profile suitable for patterning onto a microscope slide.

I. INTRODUCTION

In the body, cells adhere to the extracellular matrix (ECM) using integrin bonds. These bonds interface with cytoskeletal proteins inside the cell to help maintain its shape. Integrin is also a key part in "outside-in" signal transduction pathways which regulate tissue repair and growth [1]. In addition, it participates in "inside-out" signal transduction pathways in which the protein talin binds to integrin and causes adjacent integrin molecules to converge and form focal adhesion (FA) complexes. FAs produce stronger bonds than individual integrin bonds. FAs also act as transducers for mechanical sensing based on the traction force they experience. The exact details of how the cell uses mechanical signals in order to redistribute integrin and form focal adhesions are still uncertain and undergoing research.

An important question to answer for understanding the mechanotransduction process is how the geometry of the surface affects the formation of FAs and the traction force. Previous work has been done to determine traction forces and adhesion strengths of individual cells for microscale environments, where the functionalized surface was a circle much smaller than the cell radius [2]. In one such study, a formula relating traction force and adhesion strength was determined while assuming that the cell's bonds were most effective near the periphery of the circular adhesive patch. Then, a second equation was found which gave the traction force in terms of bond distribution and efficiency, accounting for the steady state behavior of integrin bonds on the cell's surface. The force exerted by integrin bonds decreased exponentially the farther the bond was from the edge of the adhesive patch, and the density of bonds decreased as well. This reflected the decreased mechanical advantage of bonds near the center of the cell, which would then cause the bonds to migrate towards the edges to increase their leverage, up to a saturation density.

Based on the microscale model, the adhesion strength increased with the size of the adhesive patch, but the total traction force did not [2]. The traction force was thought of as the maximum force that a set number of bonds could withstand before breaking. In addition, the number of integrin bonds was found using integrin binding analysis, which was compared to the traction force to determine that only about 10% of the bonds accounted for the the entire force, suggesting that the bonds near the cell's center did not contribute much to the total force.

A later study experimentally determined the adhesion strength in a nanoscale system, the same one for which this paper's model was created [3]. The geometry of the adhesive patches consisted of a 4 μm^2 square surrounded by eight identical islands consisting of one of more smaller squares (fig. 1). These squares were all the same size, but the experiment was repeated for designs with different numbers of squares per island and different square sizes. The adhesive patches were patterned onto a disk, each meant to hold one cell. NIH3T3 murine fibroblasts were used in this experiment. The disk was spun against a fluid flow, subjecting varying levels of shear stress depending on the distance from an adhesive path to the disk's center. This way, the regions where cells detached could be recorded and the adhesion strength could be found by determining the point were half of the cells would detach.

The nanopatterned experiment yielded interesting results, namely that designs with the same square sizes yielded the same adhesion strength regardless of the number of squares per island. Conversely, designs with identical total areas but different numbers of squares per island and different square sizes yielded different adhesion strengths. This suggested that the size of the nanoscale squares was more important in determining the adhesion strength than the total area. It was also found that for squares of side length 250 μm, stable integrin bonds did not form at all, leaving all the bonds to form in the center square.

This paper aimed to model the effects these different nanoscale geometries on the adhesion strength and trac-
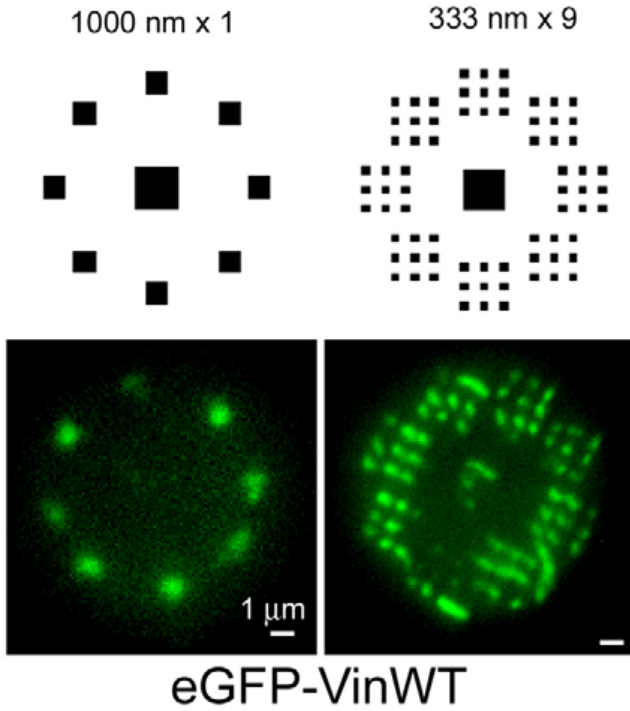
FIG. 1: Example nanopatterns used to measure cell adhesion strengths. Fibronectin is stained with fluorescent protein to image bond locations [3].

FIG. 2: Cross section of cell with radius R_c adhering to a surface while exposed to fluid flow with shear stress τ^s. The force due to the shear flow is F^s which is counteracted by the bond forces in the x direction F_b^x. The force per bond is σ and the separation distance between the cell and floor is s. [4].

tion force in order to explain these results for a nanoscale pattern. The models used for microscale systems were not adequate here because the adhesive patch was no longer just a circle, and the squares were small enough to start reaching the limits of areas suitable for integrin binding.

II. THEORY

Each cell on the nanopattern is under mechanical equilibrium unless the fluid shear stress is large enough to dislodge it. When shear stress from the fluid is just enough to balance adhesion strength, half of the cells exposed to that stress are dislodged from the nanopattern on average. This equilibrium (fig. **??**)can be split into a force balance equation in the x-direction in eq. 1 and a torque balance equation in the z direction in 2.

$$0 = F_s + F_b^x \qquad (1)$$

Because the nanopatterns were not radially symmetric and were placed on a spinning disk, the effects of the direction of fluid flow were important to consider. As a result, the torque exerted by the bonds were averaged over all the possible angles of fluid flow.
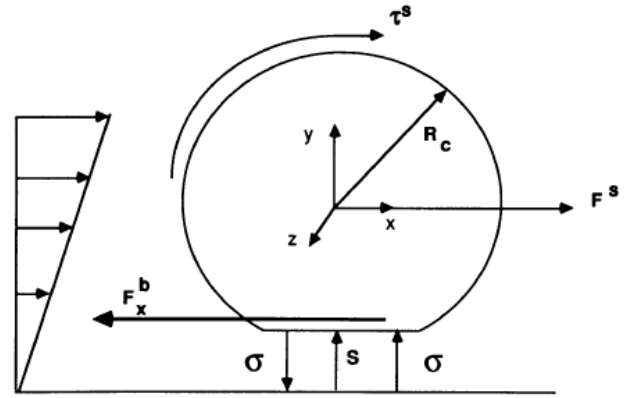
$$0 = \tau_s + F_b^x R_c + \frac{1}{2\pi} \int_0^{2\pi} \int_0^{2\pi} \int_0^{r(\theta)} \sigma N_b |r \cos{(\theta - \alpha)}| \, \mathrm{d}r\mathrm{d}\theta\mathrm{d}\alpha \qquad (2)$$

The torque integral was handled by splitting it into many different sections due to the discontinuous geometry of the nanopattern and due to the absolute value dependence on angle. The integral was split into different terms for each square in the pattern. These integrals were further split into four parts, one for each of the squares' edges. Each side's integral was split into three parts in order to take into properly account for the absolute value function for different values of θ and α. Since the torque needed to be integrated over the square itself and every term integrated from the origin to an edge, terms were negated for edges that were between another edge and the origin.

Due to the large number of integrals required to find the total torque, the general case for a square in the first quadrant was solved analytically and the result was evaluated programmatically for a quarter of the squares in the nanopattern. A quarter of the middle island was included. Then the final result was multiplied by four, taking advantage of the four-way symmetry of the nanopatterns.

Equation eq. 2 can be rearranged so that the result of the integral is a force in the y direction times a constant k that is related to the moments in the geometry.

$$F_b^y = -k(\tau_s + F_b^x R_c) \qquad (3)$$

The total traction force is given by combining its components:

$$F_t = \sqrt{(F_b^x)^2 + (F_b^y)^2} \qquad (4)$$

Equations for the total force and torque on a sphere next to a wall exposed to a steady fluid flow were derived in previous work [5] [6]. They depend on experimentally determined parameters F^s and τ^s, respectively, as well as on the fluid's dynamic viscosity μ and shear rate $\dot{\gamma}$, and the separation between the sphere and wall S. In the case of cell adhesion, S is much smaller than R_c. The constant values were used in the limiting case where R_c greatly exceeded s, $F^s = 1.7$ and $\tau^s << F^s$.

$$F_s = 6\pi\mu R_c^2 \dot{\gamma} F^s (1 + \frac{S}{R_c})(\frac{S}{R_c}) \qquad (5)$$

$$\tau_s = 4\pi\mu R_c^3 \dot{\gamma}\tau^s (\frac{S}{R_c}) \qquad (6)$$

Finally, the above equations can be combined with the torque balance equation to give the total traction force F_T in relation to the shear stress $\tau = \mu\dot{\gamma}$.

$$F_T = 32R_c^2 \tau \sqrt{1 + (kR_c/a)^2} \qquad (7)$$

A second equation was used to determine the traction force based on biological factors, such as the number and distribution of integrin bonds and the presence of focal adhesions. The force of a single bond is f, the number of integrin bonds in the center square is B_i, the number of integrin bonds outside the center square is B_o, and the fraction of integrin bonds that are associated with FAs is χ. The middle square's integrin bonds do not contribute to the force unless they are associated with FAs because integrins not bound in FAs would not stop the cell from peeling away from the substrate from the outside in and detaching that way. Bonds in FAs, on the other hand, must all be broken at the same time in order for the cell to detach, so these bonds would help the cell anchor itself more strongly.

$$F_T = fB_c\chi + fB_o \qquad (8)$$

III. METHODS

A. AutoCAD nanopatten model

In order to perform future cell adhesion studies with individual cells separated, I designed a 2-D nanopattern using AutoCAD (fig. 3). This pattern would include nanoislands in clusters that are 2.5 μm in length and 10 μm apart. Unlike the previous studies where the adhesive area was smaller than the cell and the adhesive pads
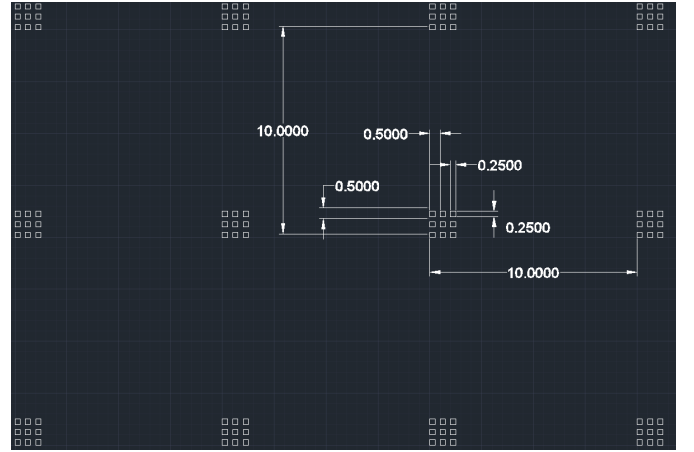

FIG. 3: AutoCAD design of nanopattern for adhering cells. Dimensions are all in micrometers.

were well separated, this design's 10 μm separation would induce cells to spread out and flatten out to cover a large surface area rather than stay in a spherical shape. The design in its entirety covers a 2.5 mm x 2.5 mm area with 500 x 500 adhesive pads, enabling simultaneous imaging of thousands of cells.

This design would likely be created on a glass microscope slide for imaging. The square islands would be imported from AutoCAD and used to make a pattern with nanoscale roughness in the squares to aid in the application of fibronectin for cell adhesion. The actual device has not been fabricated yet.

B. Model Solutions

The various nanopattern geometries were translated into a matrix of polygon vertices using MATLAB. This way, different island lengths and numbers of islands per cluster could be used as inputs to programmatically generate the pattern. Only the top right quarter of each pattern was calculated in this way. The symmetry of the designs allowed a reduction in computation time by calculating results for a quarter of the design and multiplying the results by four at the end. This program was also quite adaptable, taking in an arbitrary square size and number of squares per cluster to create the pattern.

MATLAB was also used to calculate the adhesion strength and adhesion force for each geometry. Although integration was done by hand, the program was necessary to input the coordinates of each of the endpoints on the edges into the pre-calculated integrals.

The traction force due to the various integrin bonds was calculated with eq. 8. Here, the value of .33 was used for χ based on past research with the same cell type, NIH3T3 murine fibroblasts [2]. The bond strength f was set to 100 pN, also based on past research [2]. The total number of bonds was 3000, based on integrin binding data collected on NIH3T3 cells [7]. The number
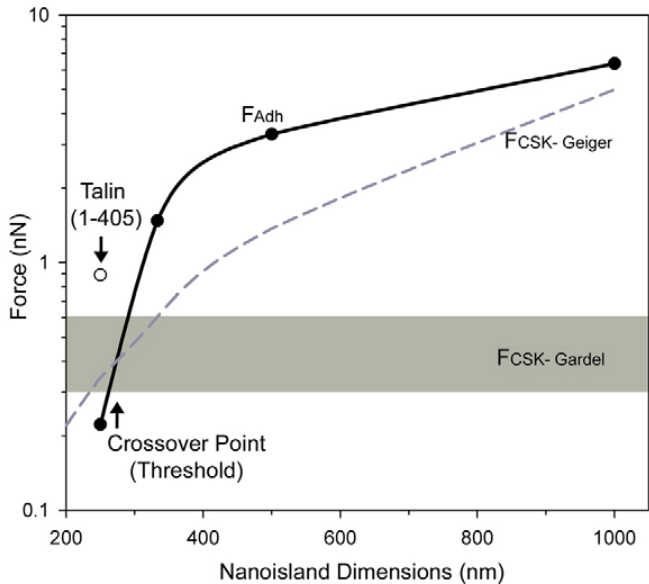
FIG. 4: Adhesion force and cytoskeletal force generated by islands of different sizes. Stables bonds form only when adhesive force exceeds the cytoskeletal force pullin on the bond [3].

of bonds was also scaled based on the expected adhesion force on the nanoisland due to the effect of size. This was done with an experimentally derived force curve obtained in [3] (fig. 4). This curve would help accound for the uneven distribution of bonds inside each square as well, where fewer bonds were seen near corners [3].

The scale factor k relating adhesion strength and traction force were found using eq. 7 and the specific geometry files for each nanopattern. The integrals in eq. 2 were calculated for every edge in the pattern. The scale factor and traction force were then used to find the adhesion strength. The cell radius R_c used a typical value for a round NIH3T3 cell, 7.5 μm.

IV. RESULTS

The geometries under investigation were successfully recreated programmatically, making it very simple to create new patterns just by inputting a square edge length and number of squares per cluster (fig. 5). Although only the coordinates in the top right quadrant of each design were calculated, the resulting pattern area was simply multiplied by four to produce accurate results for the full pattern.

For each of the nanopattern designs, the total traction force was calculated and plotted against the area of the entire design, including the center island (fig. 6). Different designs were grouped together based on the size of their nanoislands. Likewise, the adhesion strength of the same designs were grouped and plotted (fig. 7). The adhesion strength plot can be compared with a similar

one with data from the spinning disk experiment.

V. DISCUSSION

The model was able to replicate the results obtained in the spinning disk with nanopatterns experiment from [3]. It showed that the nanopattern's total area was not the main distinguishing factor between different designs in terms of their adhesion strengths. Rather, the side lengths of the individual squares had a more pronounced effect (fig. 7). Three different geometries, the 1000 $nm \times$ 1, 500 $nm \times$ 4, and 333 $nm \times$ 9 designs all had the same total area but different adhesion strengths. The same could be said for the 500 $nm \times$ 1 and 250 $nm \times$ 4 designs. This can be explained by the fact that these geometries did not have the same bond distribution or moment distribution. Designs with bigger islands had a more even bond distribution according to the model, while designs with smaller islands had fewer bonds on the smaller islands and more bonds in the center island because it would be harder for the cell to form stable FAs on small areas. The bonds in the nenter island had a smaller mechanical advantage, meaning the adhesion force was smaller overall for designs with smaller islands. This result was seen in previous studies as well [3].

At the same time, designs which had the same island side generally had similar adhesion strengths regardless of the number of islands. This is related to the fact that although the traction force was larger for designs with more islands, so was the scale factor k between ahdesion strength and traction force because the total moments were greater. As a result, the adhesion strengths were similar. For 250 nm squares, another factor was that the number of bonds in the small squares was very low, making the squares contribute little to the traction force and to the scale factor k. The system then behaved almost as if only the center island existed, regardless of the number of 250 nm islands present.

Interestingly, the model predicted the total adhesion strength to vary among the various geometries (fig. 6), wheras for the microscale system, it remained at a constant 200 nN for circular adhesive pads of varying sizes and with 3000 bonds [2]. This could be due to the fact that for circular pads, the force was modeled to decay exponentially farther from the edge. In contrast, for the nanopattern, every square had edges touching the fluid and the distribution of force was not as simple as an exponential. Each different design behaved differently in its distribution of bonds, especially because designs with smaller islands tended to saturate their outer squares, thus having more bonds in the middle square than larger designs.

Differences between the measured results and the ones obtained by the model could be accounted for in the assumptions made in the model. The model assumed that all bonds break at the same time and do not reform after the cell starts to be dislodged. Also, squares were as-
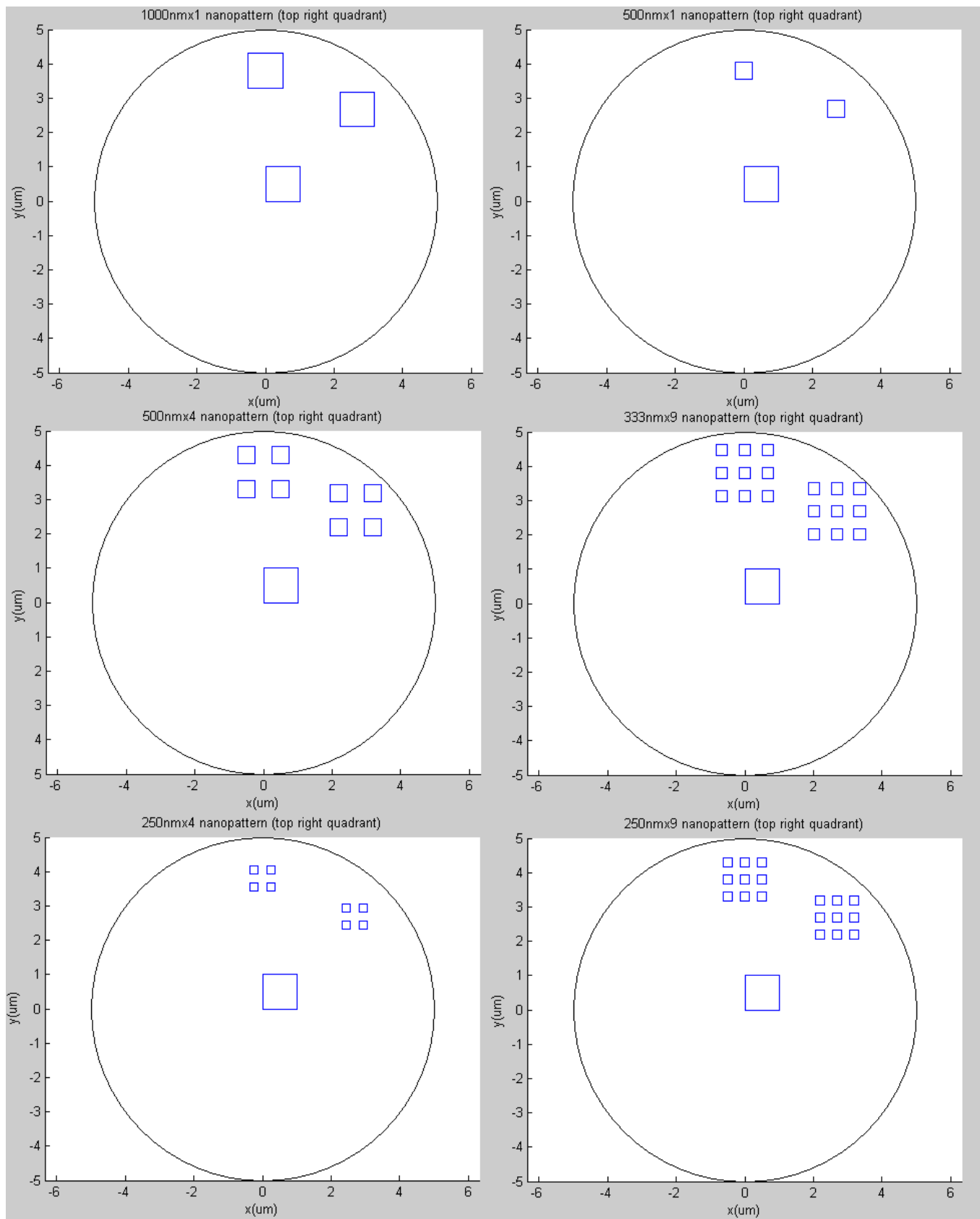
FIG. 5: Selection of nanopatterns created programmatically. Force and adhesion strength calculations were multiplied by four to include the entie design.
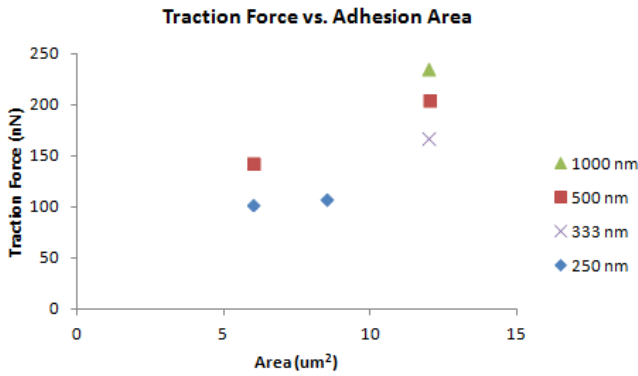
Traction Force vs. Adhesion Area

FIG. 6: AutoCAD design of nanopattern for adhering cells. Dimensions are all in micrometers.

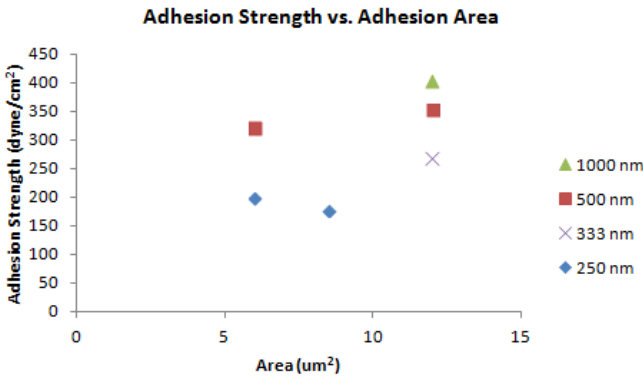**Adhesion Strength vs. Adhesion Area**

FIG. 7: AutoCAD design of nanopattern for adhering cells. Dimensions are all in micrometers.

sumed to have the same number of bonds as each other except for the center square, but in experiments, it was often the case that the squares near the edges had somewhat fewer bonds, perhaps because it was hard for bonds to withstand the shear flow on the few outermost squares [3]. These details were not expected to have impacted the results greatly.

In the future, the model can be augmented with a more quantitative explanation of the traction force generated by nanoislands with varying sizes. Another improvement could be applying this model to geometries different from the one used in the spinning disk experiment. As long as the geometry can be decomposed into squares and converted into a file containing all the vertices, the approach used by this paper could be used to derive the traction force and adhesion strength.

VI. REFERENCES

[1] Hynes, R. O. 2002. Integrins: bidirectional, allosteric signaling machines. Cell, 110(6), 673-687.
[2] Gallant, N. D., & Garca, A. J. (2007). Model of integrin-mediated cell adhesion strengthening. Journal of biomechanics, 40(6), 1301-1309.
[3] Coyer, S. R., Singh, A., Dumbauld, D. W., Calderwood, D. A., Craig, S. W., Delamarche, E., & Garca, A. J. (2012). Nanopatterning reveals an ECM area threshold for focal adhesion assembly and force transmission that is regulated by integrin activation and cytoskeleton tension. Journal of cell science, 125(21), 5110-5123.
[4] Hammer, D. A., & Lauffenburger, D. A. (1987). A dynam-

ical model for receptor-mediated cell adhesion to surfaces. Biophysical journal, 52(3), 475-487.
[5] Goldman, A. J., Cox, R. G., & Brenner, H. (1967). Slow viscous motion of a sphere parallel to a plane wallI Motion through a quiescent fluid. Chemical Engineering Science, 22(4), 637-651.
[6] Goldman, A. J., Cox, R. G., & Brenner, H. (1967). Slow viscous motion of a sphere parallel to a plane wallII Couette flow. Chemical Engineering Science, 22(4), 653-660.
[7] Gallant, N. D., Michael, K. E., & Garca, A. J. (2005). Cell adhesion strengthening: contributions of adhesive area, integrin binding, and focal adhesion assembly. Molecular biology of the cell, 16(9), 4329-4340.